Heliyon 7 (2021) e07120

Contents lists available at ScienceDirect

Heliyon

journal homepage: www.cell.com/heliyon

Research article

Simultaneous quantification of Cd(II) and Pb(II) in surface marine sediments using Ag–Hg and Ag–Bi nanoalloys glassy carbon modified electrodes

Danny Valera [b], Lenys Fernández [a,*], Gema González [c,e], Hugo Romero [d], Omar Martínez [d], Patricio J. Espinoza-Montero [a]

[a] Pontificia Universidad Católica del Ecuador, Escuela de Ciencias Químicas, Quito, 17-01-2184, Ecuador
[b] Universidad Simón Bolívar, Departamento de Química, Caracas, 1080-A, Venezuela
[c] Yachay Tech University, School of Physical Sciences and Nanotechnology, Urcuqui, 100119, Ecuador
[e] Instituto Venezolano de Investigaciones Científicas, Centro de Ing. de Materiales y Nanotecnología, Caracas, 1020-A, Venezuela
[d] Universidad Técnica de Machala, Facultad de Ciencias Químicas y de la Salud, Machala, 070151, Ecuador

ARTICLE INFO

Keywords:
Bimetallic nanoparticles
ICP-OES spectroscopy
Modified electrodes
Pb and Cd anodic stripping voltammetry

ABSTRACT

The evaluation of glassy carbon (GC) electrodes modified with a Nafion (Nf) film and doped with nanoalloys (Nys) deposits of Ag–Hg and Ag–Bi and their application to determination of Cd (II) and Pb(II) in marine sediments, is described. Deposited Ag–Hg and AgBi Nys have a size of approximately ~80 nm dispersed and embedded inside the booths of the Nf net, while other of them remained on Nf net surface. For the AgBiNysNf-GC electrode, a detection limit (DL), 3 s criterion, slightly higher than for the AgHgNysNf-GC modified electrode was obtained. Accuracy of measurements was asserted by comparison with quantification of Cd and Pb in three sets of marine sediments samples previously analyzed by inductively coupled plasma optical emission spectroscopy (ICP-OES). The values of the standard deviation and the coefficients of variation are very low, and also comparable between the different determinations.

1. Introduction

Sedimentation is defined as the process by which a solid material in suspension and in motion is deposited. Characteristic examples of this phenomenon occur when a solid material in suspension transported by a stream of water is deposited at the bottom of a river, sea, ocean, artificial channel, or a device specially built for this purpose [1]. Heavy metals comprise a category of pollutants of great interest for the study of coastal waters, due to their highly recognized toxic effects at different levels of biological organization, as well as their rates of anthropogenic mobilization towards the sea, which in some cases equal or exceed natural mobilization [2]. The chemistry of heavy metals in aquatic environments is a product of the equilibrium between various components; the most important of all is water followed by aquatic sediments. Marine sediments are one of the main reservoirs of heavy metals, therefore constituting the secondary pollution source in the marine environment [3]. High concentrations of heavy metals present in surface sediments of coastal areas, altered by anthropogenic activities, are closely related to the particles' size and the amount of organic matter present in the sediment, changing the ecological and biogeochemical balance of the ecosystem [4]. In this sense, the determination of metals in marine sediments is a good indicator of the origin of pollutants in the environment and the impact that these can produce on marine biota [5]. Heavy metals are easily transported to coastal areas, in suspended material, through rivers as the primary means of transport [6]. Hence, coasts influenced by rivers are one of the most sensitive ecosystems to be affected by heavy metals, which, when in contact with the marine area, undergo processes that allow their accumulation in sediments, whose bioavailability has a direct action on the aquatic species that accumulate high concentrations with chronic effects on their populations. In Ecuador, various ecosystems are affected by the pressure of human activities, generating a great environmental problem of contamination with heavy metals, especially in coastal marine ecosystems. These ecosystems have great importance for being generators of biomass of species of great nutritional value, which tend to become contaminated by the sedimentation of pollutants; that has biomass as its final destination. In particular, the Bajo Alto commune, in the southern province of El Oro, Machala-Ecuador, is home to about 450 families, most of whom live from fishing. The problem is that this site, with great tourist potential, has the hydrographic influences of the Jubones, Guayas and Pagua rivers, all three of great importance

* Corresponding author.
E-mail address: lmfernandez@puce.edu.ec (L. Fernández).

https://doi.org/10.1016/j.heliyon.2021.e07120
Received 29 January 2021; Received in revised form 8 April 2021; Accepted 17 May 2021

due to their flow, extension of the basin and the agricultural and mining activities that take place around them. Due to these anthropogenic activities, there could be presence of heavy metals in the sediments of the study area, which could cause environmental damage to the mangrove ecosystem and to the inhabitants of the commune and fauna that inhabit this place. Because of its persistence in the environment, toxicity and ability to be incorporated into the food chain [1], heavy metals such as cadmium (Cd) and lead (Pb) are considered serious pollutants of aquatic ecosystems. They also cause serious damage at the cellular level, given their ability to denature proteins and be assimilated by phytoplankton and filtering organisms.

Many catastrophic events for human health have occurred due to Hg, Cd and Pb poisoning resulting from seafood ingestion, which has increased interest in monitoring heavy metals in the marine environment. The main thing to face this problem is understanding the physical, chemical, and biological behavior of metals in marine systems and using this knowledge to propose research programs when pollution problems arise [7]. For this, sensitive, versatile and portable analytical methodologies and techniques are needed that are easy to use and access for the personnel who measure the metal content in this type of sample. Therefore, the main interest of the present research was the electrochemical determination by Anodic Stripping Voltammetry (ASV) of Cd and Pb in marine sediment samples using vitreous carbon electrodes mediated with Nafion films which contain Hg–Ag and Bi -Ag nanoalloy. In most cases, Hg film based sensors are preferred due to their excellent characteristics for stripping [8, 9, 10]; however, their toxicity makes them unsuitable for designing this type of device [11]. Bi has been proposed as a metal alternative to the Hg to produce friendlier electrodes. Bi-modified electrodes, a more environmentally friendly element, have been reported as an alternative material due to their electrochemical attractiveness, characteristics that include reproducible stripping behavior, wide linear range, and good signal/background ratio [12, 13]. On the other hand, Bi nanoparticles have proven to be highly sensitive and reliable modifiers for detecting heavy metal traces when used in conjunction with ASV. In the present work, we compare the use of the AgHgNysNf-GC and AgBiNysNf-GC modified electrodes to determine Cd and Pb in samples of superficial marine sediments of the Lower Alto-Ecuador commune.

2. Experimental

2.1. Reagents

Nafion, 5 % (w/w), from Aldrich; $BiNO_3{\cdot}5H_2O$ (98 %), $Cd(NO_3)_2$ (99.5 %), $Pb(NO_3)_2$, 99.5 %, and H_2O_2, 6 % (w/w) from Merck; $AgNO_3$ (99.8 %), HNO_3 (65 %), CH_3COOH (99.8 %) and ethanol (99.8 %), were purchased from Riedel-de Haën; KOH (87.8 %) from J.T. Baker; NaOH (98 %) from Eka Nobel; CH_3COONa (98 %), dimethylformamide (DMF) from Sigma and marine sediment reference material PACS-2 (National Research Council of Canada). Solutions for the electrochemical experiments were prepared using distilled/deionized, 18 MW cm^{-1}, Millipore water.

2.2. Instrumental

Princeton Applied Research, Galvanostat/Potenciostat (273A model) controlled by the 270/250 Research Electrochemistry Software 4.23, a reaction cell (15 mL) with one compartment and three electrodes. Electrochemical impedance spectroscopy (EIS) measurements were carried out using Bio-Logic SP200 Potentiostat interfaced to a computer system with EC-Lab software V11.26.The modified electrodes were used as working electrodes, Ag/AgCl electrodes as reference, and platinum wires were the counter electrodes. Atomic absorption experiments were carried out using inductively coupled plasma optical emission spectroscopy (ICP-OES). Determinations were achieved by means of a PerkinElmer, model Optima 2100DV, computer-controlled by the Win Lab 32, software 5.00. Scanning electron microscopy (SEM) was performed using a PHENOM PROX tabletop scanning electron microscope, and for force microscopy (AFM) analyses, A PARK SYSTEMS equipment (NX10) was used.

2.3. Preparation of modified electrodes

Previously reported procedure was followed [14a, 14b, 15]: GC electrodes were firstly polished using number 2000 sandpaper and afterward using spreads of aluminium oxide powder, with decreasing particle size 1.0 μm, 0.3 μm and 0.05 μm, on a billiard table cloth. After polishing, the GC electrode was submerged in an ultrasonic bath containing distilled/deionized water for 5 min to get rid of any aluminium oxide particle loosely adhered to the GC. Five microliters of a 1 % Nf solution were cast on the GC electrode, then 3 μL of pure DMF were added. DMF was evaporated by heating at 30 °C with an air gun (electrode rotation speed: 50 rpm); then, the modified electrode was submerged, for 60 min, in aqueous solutions containing 85% Ag, 15% Hg or 85% Ag and 15% Bi. Afterward, the modified electrode was washed with distilled/deionized water. Then the metallic ions trapped in the Nf net were reduced by Coulombimetry in HNO_3 aqueous solution containing 1 mol L^{-1} KNO_3 and 0.1 mol L^{-1} at -1.2 V for 300 s.

2.4. Sample treatment

The research was carried out on the beach of Bajo Alto, which has an extension of 20 km, belongs to the Tendales parish of the El Guabo canton, 10 km from the cantonal head along the Barebones road. For this, 1 Kg of sediment was taken in triplicate at a depth of 3 m (17 M 0622165 9656403,1.94 Km South), being then stored in polyethylene bags with airtight closure, previously washed with 1 % HNO_3.The samples treatment of the marine sediment from Comuna de Bajo Alto Oro province, Ecuador and samples of standard reference material was carried out according to what was reported by Ordoñes et al. [16]. Briefly: 0.5000 g (±0.0001 g) test sample was dissolved with 5 mL of HNO_3:HF:$HClO_4$ (3:3:1) solution using 800 W microwave power for 20 min; then the resulting solutions were evaporated to a volume of 1 mL and finally brought to 25 mL with 0.05 M HCl solution. Standard addition curves for the quantification of Pb and Cd were used.

2.5. Determination of Cd (II) and Pb (II) by ASV

Pre-concentration step [14a, 14b]: 0.1 mol L^{-1}, pH 4.5, acetate buffer solution and Cd (II) and Pb (II) standard solutions were used, the reaction cell was purged with Ar flow (20 mL min^{-1}) during 5 min. With continuous agitation -1.2 V potential for 100 s was applied. Differential pulse voltammetry (DPV): scanning at 20 mV s^{-1} from -650 to -350 mV was used for the re-dissolution step. After each concentration/stripping cycle, the electrode was cleaned by application of a -200 V potential for 15 s.

2.6. Cd (II) and Pb (II) determination by ICP-OES

Analytical conditions [14b]: fuel Ar; nebulization flow 8 mL·min^{-1}; wavelength Cd 228,502 nm and Pb 217 nm; cleaning step: 15 s; calibration mode standard. Linear dynamic range for both metals 10–120 μg L^{-1}. All measurements were triplicate.

3. Results and discussion

3.1. Modified electrode's characterization

We have reported [14b], that the responses of the AgHgNysNf-GC and AgBiNysNf-GC modified electrodes agree with the response of conventional Ag–Hg electrodes and Ag–Bi electrodes respectively, indicating that both metals form amalgams with Ag on the surface of the modified electrodes. SEM images of both characters (Figure 1a) show white spots

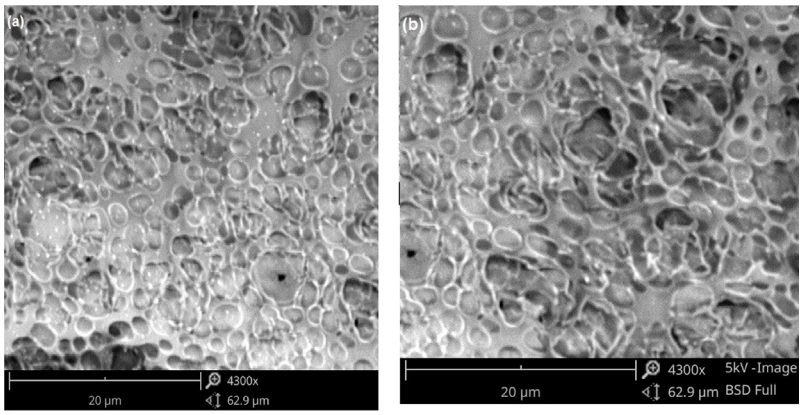

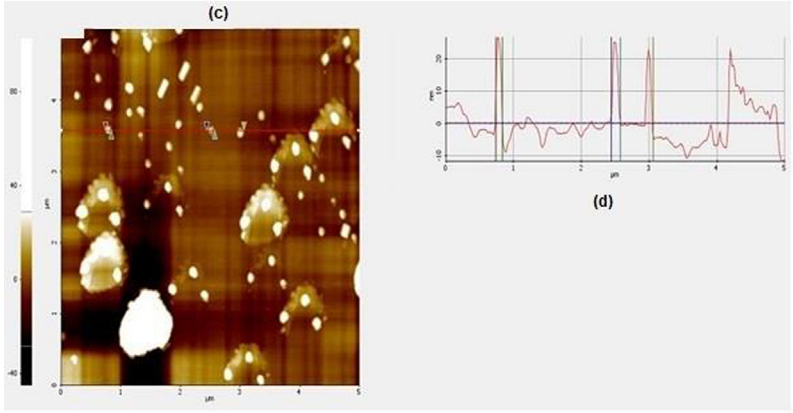

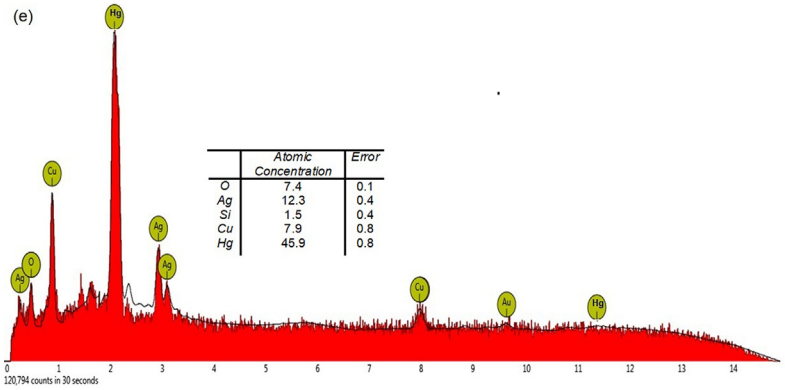

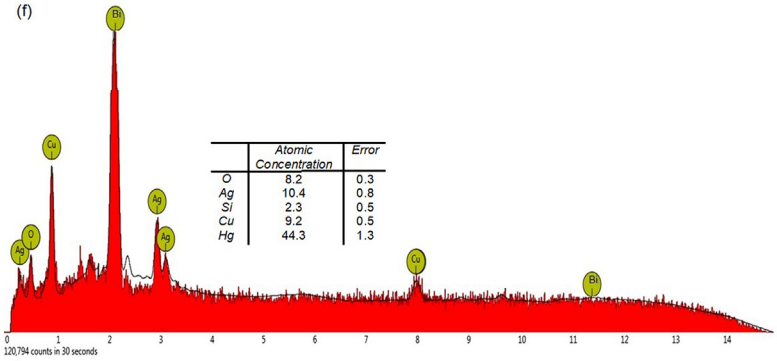

Figure 1. a) SEM micrographs of the Nf film covering the GC electrode after reducing, 60 min, the metallic ions trapped in the Nf film by Coulombimetry. Reproduced from Ref. 14b with permission from the Royal Society of Chemistry, b) SEM micrographs of Nf film, without the nanoalloys, covering the surface of the GC electrode, c) AFM images of the AgBiNysNf film at the GC electrode. Reproduced from Ref. 14b with permission from the Royal Society of Chemistry, d) AFM images scan region 5 mm, showing the average thickness of nanoalloy of the AgBi nanoparticle. Reproduced from Ref. 14b with permission from the Royal Society of Chemistry, e) Elemental analysis and results of mapping of the AgHgNysNf/GC modified electrodes, f) Elemental analysis and results of mapping of the AgBiNysNf/GC modified electrodes.

(~80 nm), nanoalloy particles inside the Nf film net. Figure 1b, shows a micrograph of the Nf film without metal nanoalloy, where the dark circles (~900–950 nm in diameter) were associated with empty spaces of Nf net. On the other hand, AFM images (Figure 1c) showed, that the Nf film rough surface has a value Ra of 140 nm and the average thickness of nanoalloy is 25 nm and 14 nm for Ag–Bi and Ag–Hg, respectively, Figure 1d [14]. Nf film's roughness modified with Ag–Hg nanoalloys is higher than with Ag–Bi nanoalloys and the Ag–Hg nanoalloys are thinner than the Ag–Bi, which we have associated with rearrangement of the Nf film as a consequence of the presence of nanoalloys. Figures 1e-f summarizes the elemental analysis of the modified electrodes, together with the results of mapping, where the presence of the expected elements in the composition of the modified electrodes is evidenced.

Electrochemical impedance spectra (EIS), from 0.1 Hz to 1×10^{-5} Hz and an applied sinusoidal perturbation of 10 mV, in the presence of dissolved oxygen were recorded. Figure 2 shows impedance spectra at -1.0 V (reduction of oxygen potential) for bare GC electrode, AgBiNysNf-GC and AgHgNysNf-GC modified electrodes. At bare GC electrode (curve a), the electron transfer resistance (Rct) at high frequency is smaller than that of the modified electrodes. Nf immobilization at the GC (curve b) produced a larger semicircle, which can be due to the limitations imposed to charge transfer by the polymer coating [15, 17]. When the bimetallic deposits were formed at the Nf/GC modified electrodes, this has an interesting effect on the shape of the impedance plots and Rct values (Figure 2 b-c). Higher impedance values were obtained at AgHgNfNysNf-GC than at AgBiNysNf-GC electrode. The AgBiNysNf-GC electrode has a lower Rct than the AgHgNfNysNf-GC. According to Brett et al. [18], the structure of polymer-coated in HgNfNysNf composite should be considered as we have corroborated [15]. The nanoparticles mercury at the AgHgNfNysNf-GC modified electrode could be a collection of nano-droplets, closely spaced. The Nf film adheres to the GC surface between the droplets, distorting the Nf film, which may explain differences between the spectra for AgHgNfNysNf-GC electrode and AgBiNfNysNf-GC electrode. The EIS spectra reveal that the bimetallic particles in the Nf film activate the coating towards electrochemical processes with resistance to electrons lower than that of the Nf/GC electrode.

3.2. Modified electrodes optimization

3.2.1. Effect of Nf film thickness

Nf film thickness can be controlled by adding to the GC electrode a given volume of solutions containing different Nf concentrations [14a]. We added fixed volumes of solutions containing Nf concentrations in the range 0.5–2.5 % (w/v). Film thickness I_{Na}, can be calculated by the formula $I_{Na} = m_{Na}/\pi R^2 d_{Na}$; where m_{Na} is the mass of Nf deposited on the electrode; d_{NA} is the density of the Nf film (1.58 g cm^{-3}) and R is the radius of the glassy carbon electrode (1.5 mm). With the addition of 5 μL of solutions containing 0.5, 1.0 and 2.5, % w/v Nf and a volume of DMF of 3 μL, films with the following thickness 2.24, 4.47 and 11.19 μm, were obtained, respectively. Nf films 2.24 μm thick and 11.19 μm gave origin to modified electrodes with impaired performance. This can be understood considering that very thin Nf films, besides being very fragile, do not provide enough space for suitable nanoparticle accommodation, and thick Nf films tend to crack due to contraction forces in the polymer. Electrodes covered with the 4.47 μm thick Nf film were stable and resistant. Experiments also showed that in an electrode with a very thin Nf film (Figure 3A-a and B-a), the stripping potential for Pb is displaced 100 mV towards the more negative values with respect to the values obtained with electrodes covered with 4.47 μm thick films (Figure 3A-b and B-b). For the case of thick films (Figure 3A-c and 3B-c), signals were broader than with the other films, with a higher probability of overlapping with signals of possible interfering ions (i.e., Cd, Cu, Fe, etc.). This fact suggests that the film has become an active and separate entity that interacts with the analytes. These results could be associated with the higher current flow resistance offered by, the thicker Nf films than the thinner ones. This shows that Nf films actively interact with the analytes through their capacity to retain the analyte on the electrode surface. The most symmetrical stripping signals were obtained with electrodes covered with 4.47 μm thick Nf films.

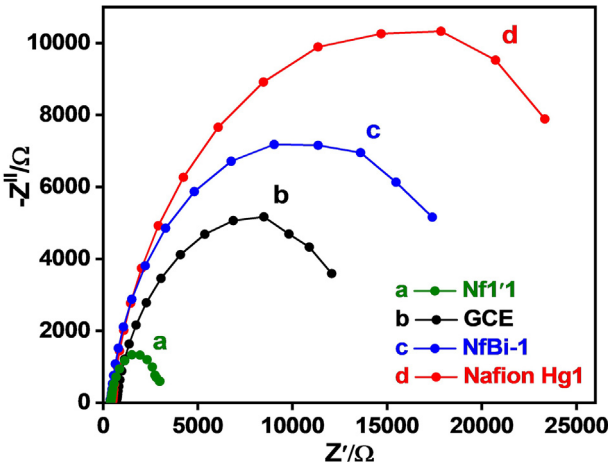

Figure 2. Nyquist plots: (a) GC, (b) AgBiNysNf/GC, (c) AgHgNysNf/GC and (d) Nf/GC. Frequency range from 0.1 Hz to 1 × 105 Hz, potential of -1.0 V, acetate buffer (pH 4.5) solution in the presence of dissolved oxygen.

3.2.2. Analyte pre-concentration potential and pre-concentration time

Effect of the pre-concentration potential for simultaneous stripping of Cd and Pb was studied in a potential range -0.8 V to -1.3 V, selected taking into consideration that effective metal pre-concentration is achieved applying potentials at least 0.3–0.5 V above the reduction potentials of the metal. Given the results reported by Valera et al. [14a, 14b], -1.2 V was chosen as the stripping potential for pre-concentration of metals.

The amount of Cd and Pb preconcentrated was found at the AgHgNysNf-GC and at the AgBiNysNf-GC electrodes as a function of time by applying a potential of -1.2 V to a 50 μg L^{-1} Cd (II) + Pb (II) solution. Accumulation was estimated by measuring the stripping charge (μC) for each metal (Figure 4). Increased amounts of each analyte at the modified electrode surface was found from 20 to 200 s. Saturation of the electrodes surface after 200 s was found. A time of 100 s, as pre-concentration time for all measurements were selected. At 100 s, the modified electrodes' sensitivity is similar or better than that reported in the literature with other electrodes after 150 s accumulation times [19, 20, 21, 22, 23, 24, 25, 26, 27], which means that the new electrodes are could save analysis time.

3.2.3. Interferences effects

In this work, the modified electrodes' selectivity was estimated by adding excesses of various possible interfering metal ions. Figure 5 shows, the DPASV peak current comparison of Cd (II) and Pb (II) in the absence (I_0) and presence (I) of interfering metal ions. We considered that a decrease of up to 10 % of the relative response in the interferer's presence can be considered acceptable. Co (II), Cr (III), Cr (VI), Fe (II) and Ni (II) ions did not significantly affect the (I_0/I) ratio. The most accentuated interference was provided by Fe (III) and Cu (II) ions, result that we have associated to surface oxide formation, formation of intermetallic compounds, or competition toward active sites on the electrode surface [28, 29].

3.3. Analytical figures of merit

Figure 6 depicts the voltammograms (a and b) and the calibration curves (c and d), for simultaneous stripping of Cd and Pb at the AgBiNysNf-GC and AgHgNysNf-GC modified electrodes. Unlike previous

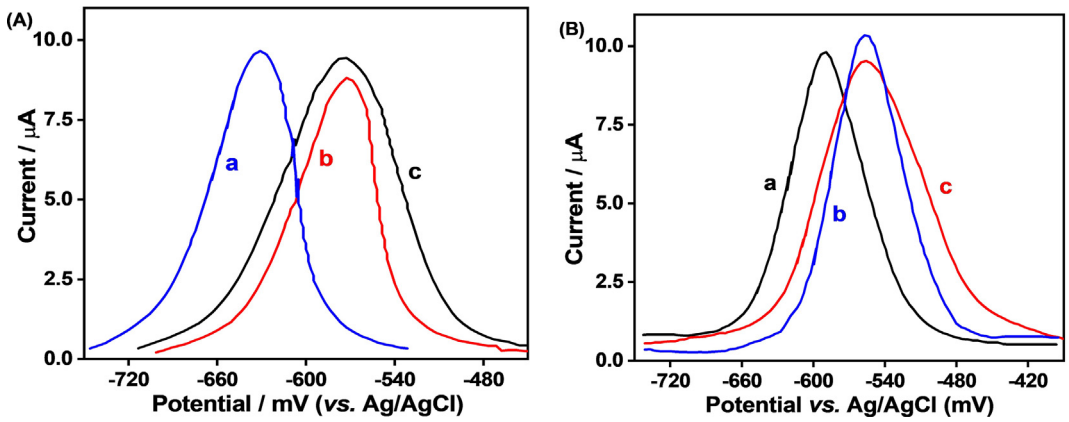

Figure 3. Displacement of the Pb signal at modified electrodes AgHgNys-Nf/GC (A) and AgBiNys-Nf/GC (B), covered with 4.47 µm thick films (A-b and B-b), towards more negative potentials going from a thicker film of 11.19 µm (A-c and B-c) to a thinner one (A-a and B-a) of 2.24 µm.

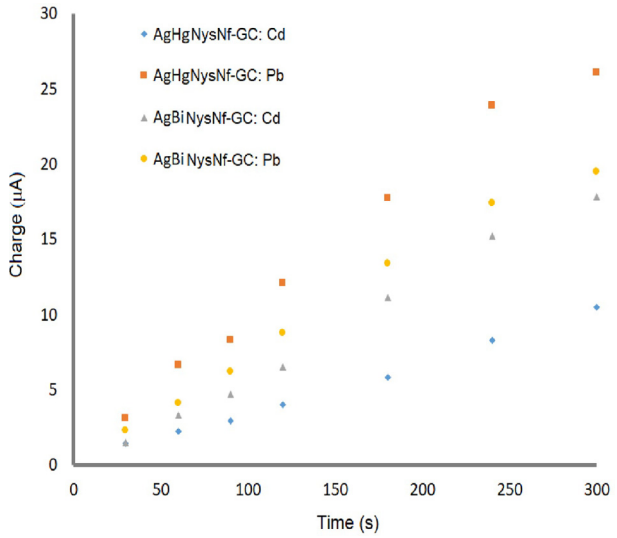

Figure 4. Charge versus analyte preconcentration time. Determination of 50 $\mu g \cdot L^{-1}$ Pb(II) by ASV.

works, we found [14], that nanoalloys of a size of 80 nm at AgBiNysNf-GC electrode the LDs calculated (3s criterion) were 0.60 µg L^{-1} for Cd (II) and 0.36 µg L^{-1} for Pb (II), n = 8, and at AgHgNysNf-GC were 0.09 µg L^{-1} for Cd (II) and 0.19 µg L^{-1} for Pb (II). Both analytes respond to quite different potentials at this electrode. The surface saturation process for both electrodes is very similar since the linear range obtained is the same for both electrodes. At AgHgNysNf-GC the sensitivity for Pb was higher than for Cd. According to the results obtained by AFM, the presence of alloyed AgHg nanoparticles increased the roughness of the AgHgNf-GC modified electrode (Figure 1c-d). This could result in a higher stripping response and generated a lower limit of detection.

Precision measurements of these modified electrodes were reported in previous works [14, 15]. The relative standard deviation (RSD) values of the twenty consecutive determinations of each metal indicated very good precision values range from 1 to 4 [30], meaning that the electrodes are mechanically very resistant and the surface modifying Nf film is strongly adhered to the GC electrode. This allows the operation of these electrodes to be very reproducible. At least 20 consecutive determinations can be performed with a single electrode.

Amounts of Cd and Pb of the PACS-2 reference material measured from three different digestions and in turn three replicates of each solution (mean ± standard deviation) were 1.984 ± 2.5 mg kg^{-1} Cd and 178.04 ± 1.8 mg kg^{-1} Pb, results that are in good agreement with the certified values 2.11 ± 0.15 mg kg^{-1} and 183 ± 8 for Cd and Pb, respectively. The Student's t-test showed that at 95 % confidence, there are no significant differences between the concentration reported for the reference material and that found using the modified electrodes proposed in this article.

Table 1 shows the comparison between AgHgNysNf-Gc and AgbiNysNf-GC electrodes and other electrodes reported in the literature. It can be seen that our results are consistent with other reports, indicating that the electrodes coating can be used to sense Cd and Pb simultaneously.

3.4. Determination of Cd and Pb in marine sediments samples

Following our main objective, the modified electrodes were applied for the determination of Cd and Pb in surface marine sediments samples

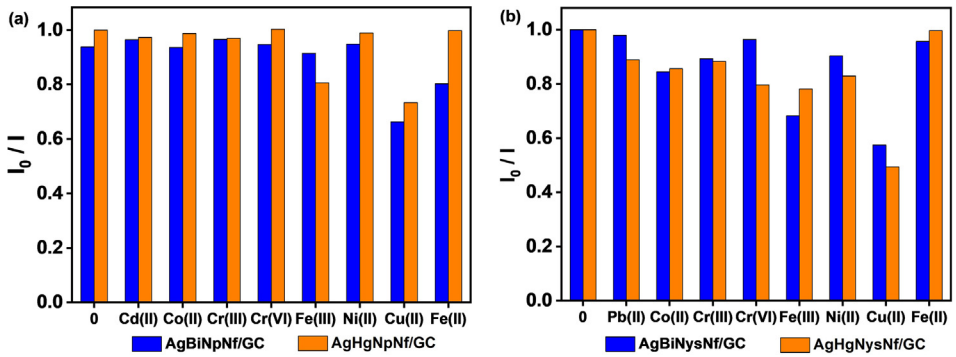

Figure 5. Effect of interfering ions (200 $\mu g \cdot L^{-1}$ each interfering metal) in the Pb (a) and Cd (b) determination (50 $\mu g \cdot mL^{-1}$ in solution). n = 6.

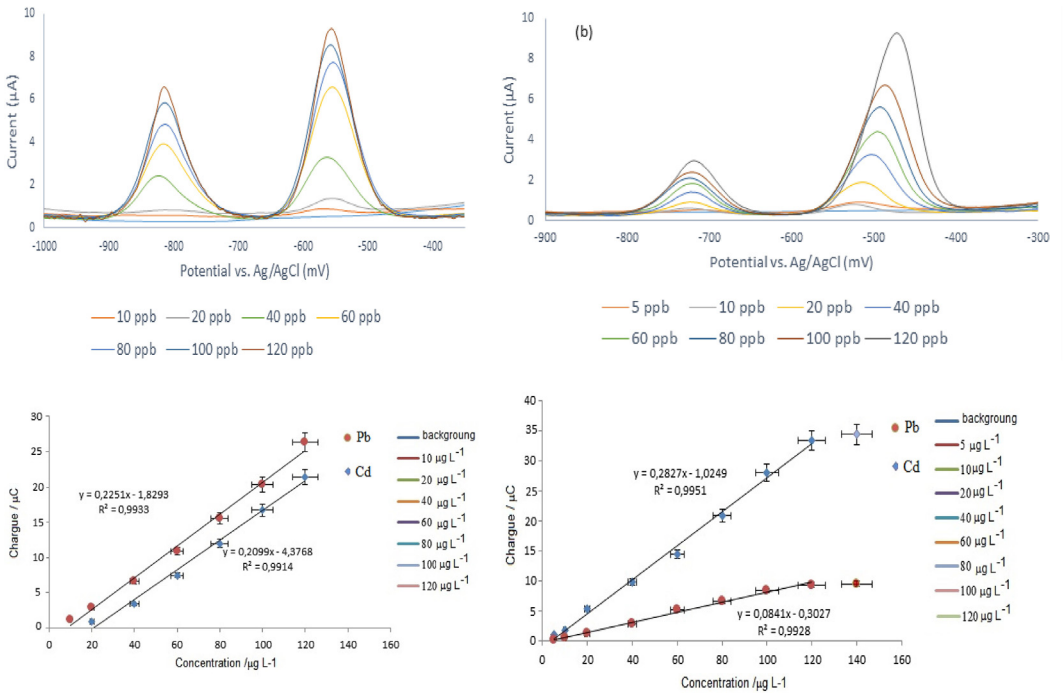

Figure 6. Anodic stripping voltammograms and the calibration curves of Pb(II) and Cd(II) at concentrations between 10-120 µg L^{-1} at: a, c) AgHgNys-Nf/GC and b, d) AgBiNys-Nf/GC. Reproduced from Ref. 14a with permission from NovaSinergia.

Table 1. Comparison of performance of the modified electrodes with other electrodes reported in the literature.

Modified Electrode	Pb detection limit (µg L^{-1})	Cd detection limit (µg L^{-1})	References
AgHgNysNf-GC	0.19	0.09	This work
AgBiNysNf-GC	0.36	0.60	This work
GR/L-cys/Bi/SPE	0.56	0.98	[31]
GQDs–NF/Gc	8.49	11.30	[20]
GSH/AuNPs/NH_2-rGO	0.38	0.09	[21]
Hg–Bi/PDAAQ/GC	3.19×10^{-4}	0.11	[32]
Nafion-Bismuth/Nitrogen/NMC/GC	0.05	1.5	[27]
$FeNi_3$/CuS/BiOCl/CPE	0.1	0.4	[33]

Table 2. R % in the ASV simultaneous determination of Cd and Pb in marine sediments samples. Concentration metal added 50 µg L^{-1}.

AgBiNysNf-GC electrode				AgHgNysNf-GC electrode		
Metal	Metal found (µg L^{-1})	Metal detected (µg L^{-1})	R%	Metal found (µg L^{-1})	Metal detected (µg L^{-1})	R%
Cd(II)	59.89 ± 2.12	11.73 ± 2.77	96.32	62.05 ± 3.43	10.79 ± 2.66	102.52
Pb(II)	69.39 ± 2.04	19.02 ± 2.15	100.74	72.13 ± 1.91	19.48 ± 2.92	105.03

Table 3. Comparison of Pb(II) and Cd(II) concentration values found in marine sediments samples by ASV using the AgHgNysNf-GC electrode with values found by ICP-OES.

Metal	Found by ASV (mg L^{-1})	Found by ICP (mg L^{-1})	Relative error, (%)
Pb(II)	19.48 ± 2.92	20.47 ± 0.025	-3.32 ± 0.06
Cd(II)	10.79 ± 2.66	11.38 ± 0.099	-5.18 ± 0.04

Table 4. Comparison of Pb(II) and Cd(II) concentration values found in sediments samples by ASV using the AgBiNysNf-GC electrode with values found by ICP-OES.

Metal	Found by ASV (mg L^{-1})	Found by ICP (mg L^{-1})	Relative error, (%)
Pb(II)	19.02 ± 2.17	18.65 ± 0.022	1.98 ± 0.07
Cd(II)	11.73 ± 2.77	11.17 ± 0.053	5.02 ± 0.01

collected from Comuna de Bajo Alto, El Oro province, Ecuador. Samples were doped with 50 μg L^{-1} of both, Cd (II) and Pb (II), and analyzed following the analytical protocol described in section 2.5. ASV methodology accuracy was checked by calculation of percentages of recovery (R %) of the two analytes, expressed as relative error, R (Table 2), and by comparison of ASV results with those obtained by inductively coupled plasma optical emission spectroscopy (ICP-OES) (Tables 3 and 4), section 2.6.

Table 2 shows that for both modified electrode, determination of Pb can be achieved with R % within 96–105 % and that the sample matrice do not represent a limitation in the simultaneous quantification of Pb and Cd.

Using the AgHgNysNf-GC electrode (Table 3), the relative error percentages obtained by comparison between both methodologies, ICP-OES and ASV, range between around -5% for the determination of Cd, and about -3% for the determination of Pb. These results say that both methodologies are appropriate for the simultaneous determination of Cd or Pb in marine sediments samples with acceptable accuracy. Similar results were obtained at the AgBiNysNf-GC modified electrode (Table 4). Regarding precision at both electrodes, expressed as relative standard deviation, RSD, it is clear that ICP-OES measurements are more reproducible than the ASV ones. The high temperatures in the core of the Ar plasma and the relatively large way the sample travels before reaching the observation zone guarantee that practically all the sample matrix is destroyed, freeing the measurements from most matrix effects. This is one reason why the ICP-OES technique has been taken as a reference for heavy element determination in complex matrix samples. Compared to the ASV ones, higher reproducibility of the ICP results was expected in accordance with the mentioned characteristics advantages of this technique. All the values obtained by ASV at AgHgNpNf-GC electrode are below those of ICP-OES; this implies that we always have errors by default which we can associate with the matrix effect at AgHgNysNf-GC electrode. However, on the electrode, this effect seems to have less influence.

4. Conclusion

Results show that the new electrodes could be useful for Pb and Cd determination in marine sediments samples with acceptable accuracy and precision. The ASV technique with the new electrodes again offers a faster, lower cost, more mobile, and easier to operate alternative. We consider the AgHgNysNf/GC electrode to be a good alternative. Although it still contains Hg, the amount of mercury is infinitesimally lower than that in a massive Hg electrode, so the electrode can be considered friendly to people and the environment. The alloyed combination in the bimetallic modified electrodes, taken as a unique entity, shows analytical characteristics not shown by any of the metals on their own. This is a very interesting area of research within electrochemistry that could deal with the nanoalloys' optical, catalytic and magnetic properties.

Declarations

Author contribution statement

Danny Valera: Conceived and designed the experiments; Performed the experiments.

Lenys Fernández: Conceived and designed the experiments; Performed the experiments; Analyzed and interpreted the data; Contributed reagents, materials, analysis tools or data; Wrote the paper.

Gema González, Patricio J. Espinoza-Montero: Analyzed and interpreted the data.

Hugo Romero, Omar Martínez: Contributed reagents, materials, analysis tools or data.

Funding statement

The work was supported by Pontificia Universidad Católica del Ecuador, Universidad Simón Bolívar Caracas-Venezuela, and Corporación Ecuatoriana para el Desarrollo de la Investigación y la Academia (CEDIA).

Data availability statement

Data will be made available on request.

Declaration of interests statement

The authors declare no conflict of interest.

Additional information

No additional information is available for this paper.

References

[1] E. Becerra Aguilar, Análisis del grado de contaminación por metales pesados en sedimentos de ecosistemas acuáticos, 2020.
[2] E.A. Gutiérrez-Galindo, G. Flores-Muñoz, V. Ortega-Lara, J.A. Villaescusa-Celaya, Metales pesados en sedimentos de la costa fronteriza Baja California (México)-California (EUA), Cienc. Mar. 20 (1) (1994) 105–124.
[3] B. Rubio, L. Gago, F. Vilas, M. Nombela, S. Garcia-Gil, I. Alejo, O. Pazos, Interpretación de tendencias históricas de contaminación por metales pesados en testigos de sedimentos de la Ría de Pontevedra, Thalassas 12 (1996) 137–152.
[4] M. Sadiq, Toxic Metal Chemistry in marine Environments, Marcel Dekker, New York, 1992, p. 390.
[5] V. Acosta, C. Lodeiros, W. Senior, G. Martínez, Niveles de metales pesados en sedimentos superficiales en tres zonas litorales de Venezuela, Interciencia 27 (12) (2002) 686–690.
[6] J. Zhang, Transport of particulate heavy metal towards the China Sea: a preliminary study and comparison, Mar. Chem. 40 (1992) 61–178.
[7] G. Martínez, Metales pesados en sedimentos superficiales del Golfo de Cariaco, Venezuela, 2002.
[8] X.S. Zhu, C. Gao, J.W. Choi, P.L. Bishop, C.H. Ahn, On-chip generated mercury microelectrode for heavy metal ion detection, Lab Chip 5 (2004) 212–217.
[9] D. Lakshmi, P.S. Sharma, B.B. Prasad, Imprinted polymer-modified hanging mercury drop electrode for differential pulse cathodic stripping voltammetric analysis of creatine, Biosens. Bioelectron. 22 (2007) 3302–3308.
[10] M.A. Ferreira, A.A. Barros, Determination of As(III) and arsenic(V) in natural waters by cathodic stripping voltammetry at a hanging mercury drop electrode, Anal. Chim. Acta 459 (2002) 151–159.
[11] D. Cargnelutti, L.A. Tabaldi, R.M. Spanevello, G. de Oliveira Jucoski, V. Battisti, M. Redin, V.M. Morsch, Mercury toxicity induces oxidative stress in growing cucumber seedlings, Chemosphere 65 (6) (2006) 999–1006.
[12] X. Pei, W. Kang, W. Yue, A. Bange, W.R. Heineman, I. Papautsky, Improving reproducibility of lab-on-a-chip sensor with bismuth working electrode for determining Zn in serum by anodic stripping voltammetry, J. Electrochem. Soc. 161 (2014) B3160–B3166.
[13] S.D. Borgo, V. Jovanovski, B. Pihlar, S.B. Hocevar, Operation of bismuth film electrode in more acidic medium, Electrochim. Acta 155 (2015) 196–200.
[14] a) D. Valera, M. Sánchez, J. Domínguez, P.J. Espinoza-Montero, C. Velasco-Medina, P. Carrera, L. Fernández, Detection of Cd (II) and Pb (II) by anodic stripping voltammetry using glassy carbon electrodes modified with Ag-Hg and Ag-Bi bimetallic alloyed, NOVASINERGIA 2 (2) (2019) 75–83. ISSN 2631-2654;
b) D. Valera, M. Sánchez, J.R. Domínguez, J. Alvarado, P.J. Espinoza-Montero, P. Carrera, L. Fernández, Electrochemical determination of lead in human blood serum and urine by anodic stripping voltammetry using glassy carbon electrodes covered with Ag–Hg and Ag–Bi bimetallic nanoparticles, Analy. Methods 10 (34) (2018) 4114–4121.
[15] C. Velasco-Medina, P.J. Espinoza-Montero, M. Montero-Jimenez, J. Alvarado, M. Jadán, P. Carrera, L. Fernandez, Development and evaluation of copper electrodes, modified with bimetallic nanoparticles, to be used as sensors of cysteine-rich peptides synthesized by tobacco cells exposed to cytotoxic levels of cadmium, Molecules 24 (12) (2019) 2200.
[16] J. Ordoñes, L. Fernández, H. Romero, P. Carrera, J. Alvarado, Electrochemical generation of antimony volatile species, stibine, using gold and silver mercury amalgamated cathodes and determination of Sb by flame atomic absorption spectrometry, Talanta 141 (2015) 259–266.
[17] C.M. Brett, D.A. Fungaro, J.M. Morgado, M.H. Gil, Novel polymer-modified electrodes for batch injection sensors and application to environmental analysis, J. Electroanal. Chem. 468 (1) (1999) 26–33.

[18] C.M. Brett, V.A. Alves, D.A. Fungaro, Nafion-coated mercury thin film and glassy carbon electrodes for electroanalysis: characterization by electrochemical impedance, Electroanalysis: Int. J. Dev. Fund. Prac. Asp. Electroanaly. 13 (3) (2001) 212–218.
[19] C. Laghlimi, Y. Ziat, A. Moutcine, M. Hammi, Z. Zarhri, R. Maallah, A. Chtaini, Analysis of Pb (II), Cu (II) and Co (II) in Drinking Water by a New Carbon Paste Electrode Modified with an Organic Molecule, 2020.
[20] J. Pizarro, R. Segura, D. Tapia, F. Navarro, F. Fuenzalida, M.J. Aguirre, Inexpensive and green electrochemical sensor for the determination of Cd (II) and Pb (II) by square wave anodic stripping voltammetry in bivalve mollusks, Food Chem. (2020) 126682.
[21] J. Mei, Z. Ying, W. Sheng, J. Chen, J. Xu, P. Zheng, A sensitive and selective electrochemical sensor for the simultaneous determination of trace Cd 2+ and Pb 2 +, Chem. Pap. 74 (3) (2020) 1027–1037.
[22] K.M. Hassan, S.E. Gaber, M.F. Altahan, M.A. Azzem, Single and simultaneous voltammetric sensing of lead (II), cadmium (II) and zinc (II) using a bimetallic Hg-Bi supported on poly (1,2-diaminoanthraquinone)/glassy carbon modified electrode, Sens. Bio-Sens. Res. 29 (2020) 100369.
[23] W. Zhang, S. Fan, X. Li, S. Liu, D. Duan, L. Leng, L. Qu, Electrochemical determination of lead (II) and copper (II) by using phytic acid and polypyrrole functionalized metal-organic frameworks, Microchimica Acta 187 (1) (2020) 69.
[24] W. Jin, Y. Fu, M. Hu, S. Wang, Z. Liu, Highly efficient SnS-decorated Bi_2O_3 nanosheets for simultaneous electrochemical detection and removal of Cd (II) and Pb (II), J. Electroanal. Chem. 856 (2020) 113744.
[25] X. Qin, D. Tang, Y. Zhang, Y. Cheng, F. He, Z. Su, H. Jiang, An electrochemical sensor for simultaneous stripping determination of Cd (II) and Pb (II) based on gold nanoparticles functionalized β-cyclodextrin-graphene hybrids, Int. J. Electrochem. Sci 15 (2020) 1517–1528.
[26] Y. Zhang, C. Li, Y. Su, W. Mu, X. Han, Simultaneous detection of trace Cd(II) and Pb(II) by differential pulse anodic stripping voltammetry using a bismuth oxycarbide/nafion electrode, Inorg. Chem. Commun. 111 (2020) 107672.
[27] L. Xiao, H. Xu, S. Zhou, T. Song, H. Wang, S. Li, Q. Yuan, Simultaneous detection of Cd(II) and Pb(II) by differential pulse anodic stripping voltammetry at a nitrogen-doped microporous carbon/Nafion/bismuth-film electrode, Electrochim. Acta 143 (2014) 143–151.
[28] M. Saénz, L. Fernández, J. Domínguez, J. Alvarado, Electrochemical generation of lead volatile species as a method of sample introduction for lead determination by atomic absorption spectrometry, Electroanalysis 22 (23) (2010) 2842–2847.
[29] M. Sáenz, L. Fernández, J. Domínguez, J. Alvarado, Electrochemical generation of volatile lead species using a cadmium cathode: comparison with graphite, glassy carbon and platinum cathodes, Spectrochim. Acta B Atom Spectrosc. 71 (2012) 107–111.
[30] Agencia para Sustancias Tóxicas y el Registro de Enfermedades (ATSDR), Resumen de Salud Pública: Plomo, 2007, p. 2014.
[31] C. Li, X. Zhao, X. Han, Simultaneous determination of trace Cd 2+ and Pb 2+ using GR/l-cysteine/Bi modified screen-printed electrodes, Analy. Methods 10 (40) (2018) 4945–4950.
[32] K.M. Hassan, S.E. Gaber, M.F. Altahan, M.A. Azzem, Single and simultaneous voltammetric sensing of lead (II), cadmium (II) and zinc (II) using a bimetallic Hg-Bi supported on poly (1,2-diaminoanthraquinone)/glassy carbon modified electrode, Sens. Bio-Sens. Res. 29 (2020) 100369.
[33] M. Malakootian, S. Hamzeh, H. Mahmoudi-Moghaddam, A new electrochemical sensor for simultaneous determination of Cd (II) and Pb (II) using $FeNi_3$/CuS/BiOCl: RSM optimization, Microchem. J. 158 (2020) 105194.